Supplementary data

S.1 Extraction of electroabsorption component from electromodulated differential absorption (EDA) data at high pump intensities

At an excitation intensity of 2 μJ/cm^2, the amplitude of pump-induced transient absorption (Fig. S1b, blue) is much lower than the EDA amplitude at the same pump intensity (Fig. S1a, blue solid curve). Thus, EDA is dominated by ground state electroabsorption, and field-induced changes of the population of excited state(s) are of minor importance at 2 μJ/cm^2. This does not apply to conditions of stronger pump flux. Fig. S1a shows EDA spectra at 500 ps at three different excitation intensities 2 μJ/cm^2, 7 μJ/cm^2, and 28 μJ/cm^2. The shift of the isosbestic point with increasing flux from 500 nm towards shorter wavelengths implies the appearance of new spectral features. EDA kinetics at 540 nm cannot be used for the determination of the electric field dynamics at higher excitation intensity as it is done for 2 μJ/cm^2 fluence. EDA amplitudes for 7 μJ/cm^2 and 28 μJ/cm^2 excitation are roughly equal at 540 nm, but it is obvious that the Stark feature in the EDA spectrum is much weaker at 28 μJ/cm^2. There is a remarkable similarity between the EDA spectrum and the differential absorption spectrum (Fig. S1, red curves) at 500 ps delay time at 28 μJ/cm^2 fluence. Our differential absorption data of $PC_{61}BM$ films in agreement with reference [1] show flat photoinduced absorption in a visible range. A positive EDA signal, which resembles a differential absorption spectrum, is most probably the result of the field-stabilized excited state of $PC_{61}BM$. The electric field reduces the relaxation rate to the ground state and this leads to the stronger induced absorption in the presence of the external field. It is still possible to get information about a decay of the electric field from EDA spectra at higher excitation intensities in spite of the appearance of a new spectral band. The whole spectra and not just one specific wavelength should be analyzed. The task consists in retrieving the ground state electroabsorption (Stark effect) contribution from EDA spectra. Purely mathematically, this can be done unambiguously if spectral constituents are orthogonal functions. Nevertheless, the unsophisticated procedure may give a result of high certainty, since field-induced changes of excited state(s) population and resulting absorption of this(ese) state(s) have a rather flat spectrum in the region of

electroabsorption. The iterative procedure described below was performed on the EDA spectrum for each time delay that gave the amplitude of EA and, consequently, the electric field as a function of time. Input data were EDA and EA spectra:

$$\frac{EDA(\lambda,t_j)+err_i}{EA(\lambda)}=\alpha_i(\lambda,t_j). \quad \text{(S.1)}$$

Initially residual err_i was set to zero, $\alpha_i(\lambda,t_j)$ are wavelength-dependent multipliers. Index *i* numerates the number of iteration and index *j* numerates the delay. The weighted average of $\alpha_i(\lambda,t_j)$ over the EA spectrum supposed to reflect the amplitude of EA:

$$\langle\alpha_i(\lambda,t_j)\rangle_{\text{weighted}}=EA_{ampl}(t_j) \quad \text{(S.2)}$$

The last step of iteration calculated residual:

$$err_i=\langle err(\lambda)_i\rangle=\langle EDA(\lambda,t_j)-EA_{ampl}(t_j)\cdot EA(\lambda)\rangle \quad \text{(S.3)}$$

The procedure was repeated until $|err_{i+1}-err_i|<\delta$, where δ is the user-defined parameter of precision. The value of $EA_{ampl}(t_j)$ obtained at the last iteration for a given t_j was used for the estimation of the electric field relying on the square law dependence between the EA and the field.

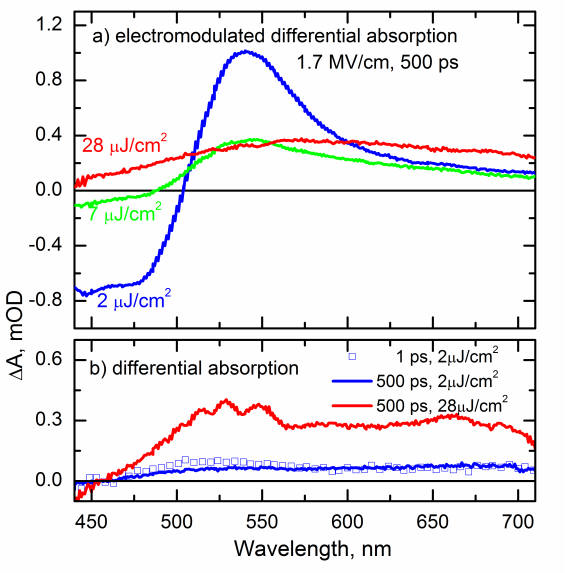

Figure S1. a) EDA spectra at 500 ps delay and an applied bias of 6 V; b) differential absorption spectra of pristine $PC_{61}BM$ film at different excitation intensities and delays as indicated in labels.

S2. Steady-state electroabsorption of MD376/$PC_{61}BM$ blend

Figure S2 shows the EA spectrum of MD376/$PC_{61}BM$ 1:1 blend film. The origin of the EA spectrum is not specific or distinctive for the purpose of the electric field and charge drift determination. The dependence of the EA amplitude on the electric field is significant. Nevertheless, we must clarify the observed phenomenon. The EA spectrum pretty much follows the second derivative of the absorption, and the amplitude of the EA signal in the visible range is proportional to the square of the electric field (insert in Fig. S2). Both features are the signature of the second order linear Stark effect [2,3]. This effect requires the non-zero dipole moment of the molecules in a ground state and MD376 according to quantum chemical calculations has a strong dipole moment of 6.2 D [4,5]. All these facts make the EA spectrum of MD376/$PC_{61}BM$ (1:1) blend evident, i.e. arising from the ground state dipole moment of randomly oriented MD376 molecules. One might expect contribution of $PC_{61}BM$ to the EA spectrum of the blend. Indeed, mismatch between EA and the second derivative of absorption is pronounced in a narrow spectral range at about 475÷500 nm, where one of the EA peaks of pristine $PC_{61}BM$ is located. It should be noted that the peak amplitude of EA of the blend is by about three times higher than that of pristine $PC_{61}BM$ and the effective thickness of $PC_{61}BM$ in the 1:1 blend by weight is approximately two times less. Thus, it is not surprising that EA of $PC_{61}BM$ makes a small contribution to the EA of the blend film. Likely, the EA spectrum of MD376/$PC_{61}BM$ blend is the superposition of the quadratic Stark effect in both constituents and of the second order linear Stark effect in MD376, where the latter contribution dominates. As long as the amplitude of both effects has the same quadratic dependence on the electric field it is not necessary to disentangle these two effects in order to determine the field dynamics.

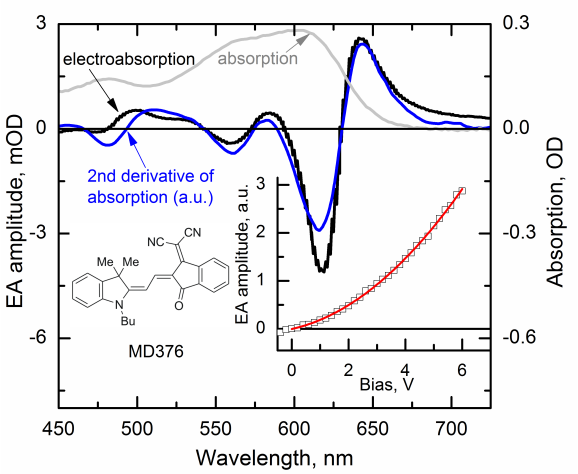

Figure S2. Steady-state electroabsorption spectrum, absorption spectrum and second energy derivative of absorption spectrum of MD376/$PC_{61}BM$ (1:1 ww) blend film. Insert shows the electroabsorption amplitude dependence on applied voltage fitted by parabolic function.

S3. Calculation of the electron-hole separation distance and the average charge carrier mobility in MD376/$PC_{61}BM$ blend

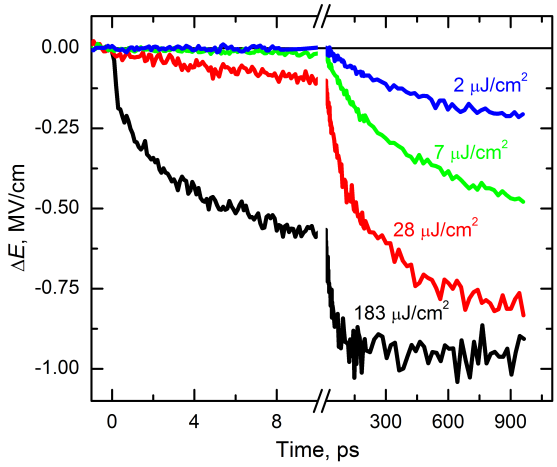

Figure S3. Time evolution of the electric field strength in MD376/$PC_{61}BM$ (1:1 w/w) blend device under an applied voltage of 6 V (1.7 MV/cm) and excitation fluences of 2 μJ/cm^2 (blue), 7 μJ/cm^2 (green), 28 μJ/cm^2 (red), and 183 μJ/cm^2 (black).

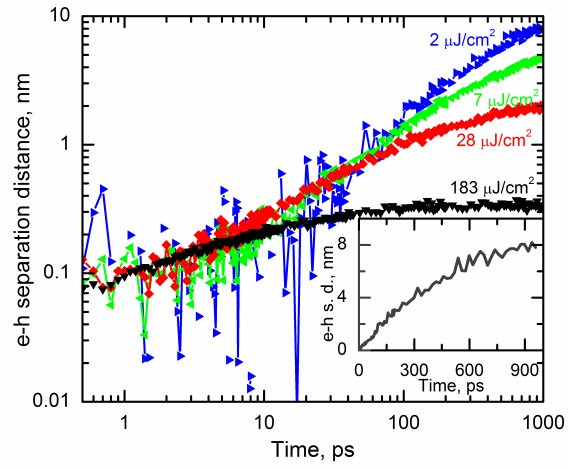

Figure S4. Average electron-hole separation distance in the direction of the field as a function of time in MD376/$PC_{61}BM$ (1:1) blend device at applied voltage of 6V (1.7 MV/cm) and excitation intensity of 2μJ/cm^2 (blue), 7μJ/cm^2 (green), 28μJ/cm^2 (red) and

183μJ/cm^2 (black). Insert shows a separation distance (not affected by screening of the field) combined from the measurements at different intensity.

Figure S3 shows kinetics of the electric field in MD376/$PC_{61}BM$ (1:1 w/w) blend obtained at the applied bias of 6 V and identical excitation conditions as in case of pristine $PC_{61}BM$. These kinetics were used to calculate the charge carrier mobility as shown below.

Writing analytical expression, which describes a decay of the field as a function of time, requires presumption regarding the drift speed of charge carriers, *i.e.* mobility. Reduction of the field in a film is a result of counteracting electrical dipole that is created by the electron-hole separation in a direction parallel to the electric field. Thus, the decay of the field might be expressed as a function of the average separation distance $\langle l(t) \rangle$ of the electron-hole pair in the direction of the electric field without assuming a mobility as a constant. If charge generation is homogeneous, expression, which accounts for charge extraction, takes this form:

$$\Delta E(t) = \Delta E_{total} \frac{1}{d} \cdot \left(2 \cdot \langle l(t) \rangle - \frac{\langle l(t) \rangle^2}{d} \right) \qquad \text{(S4)}$$

Where d is the thickness of the active layer. Expressing $\langle l(t) \rangle$ leads to:

$$\langle l(t) \rangle = d \left[1 - \sqrt{1 - \Delta E(t) / \Delta E_{total}} \right]. \qquad \text{(S5)}$$

Figure S3 shows time-dependence of $\langle l(t) \rangle$ obtained from the experimental data of the field dynamics according to (S5). We should note that the separation distance presented in this figure does not reflect the absolute distance between an electron and a hole. It is the average component of the separation in the direction of the applied field. The initial charge separation is governed by the disordered morphology of MD376/$PC_{61}BM$ blend. The electric field makes only weak influence. As a consequence, the charge pairs separate in random directions yielding minor component along the field. Results at a different pump intensities are complementary. Low pump intensity data are noisy at early

time because the same electron-hole displacement causes a weaker decrease of the electric field at low carrier concentration, whereas the separation distance starts to saturate because of the space charge screening effect at high intensity. In order to obtain $\langle l(t) \rangle$ with reasonable accuracy and unaffected by the field screening in all time domains we combined it from data measured at different excitation intensities. Insert in Fig. S3 shows the obtained result on a linear scale. Time intervals of 0-4 ps, 6-30 ps, 30-80 ps and 80-1000 ps are assembled from 183 μJ/cm^2, 28 μJ/cm^2, 7 μJ/cm^2 and 2 μJ/cm2 data, respectively. Continuous interconnection of the data confirms the applicability of a linear extrapolation of extracted charge as a measure for the photogenerated charge density under high excitation conditions. If mobility was time-independent, the separation distance would follow a straight line with time before the extraction of substantial amount of charge, i. e. while the separation distance is much smaller than the film thickness. It is clear that a slope of the curve (insert Fig S3) decreases with time and it is not a consequence of the space charge effect because the electric field decreases by less than 15 % after 1 ns at excitation intensity of 2 μJ/cm^2. This must be a consequence of decreasing mobility. Instantaneous mobility averaged over both types of carriers ─ electrons and holes ─ can be obtained by calculating temporal derivative of the electron-hole separation distance. It is not an easy task because of the experimental noise. Smoothing procedures or approximations by series of elementary functions have to be applied in order to accomplish this task and the result depends on the chosen path. Thus, we present running average of the mobility ($\overline{\mu(t)} = E^{-1} \cdot \Delta\langle l \rangle / (t - t_0)$) in the main text, and not an instantaneous mobility $\mu = E^{-1} \cdot d\langle l \rangle / dt$.

S4. Experimental setup

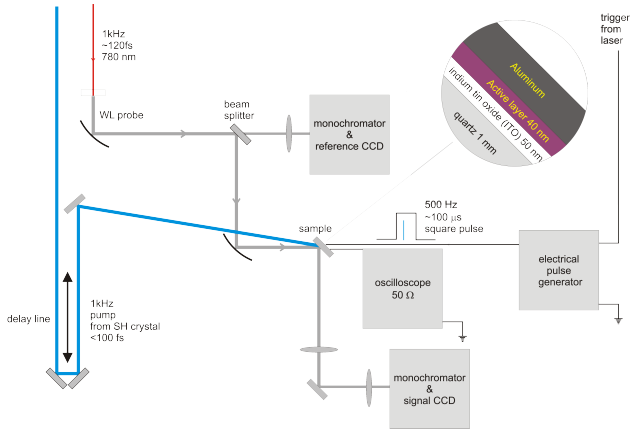

Figure S5. Scheme of experimental setup for electromodulated differential absorption measurement.

REFERENCES:

1. G. Grancini, D. Polli, D. Fazzi, J. Cabanillas-Gonzalez, G. Cerullo, G. Lanzani, Transient Absorption Imaging of P3HT:PCBM Photovoltaic Blend: Evidence for Interfacial Charge Transfer State, *J. Phys. Chem. Lett.* 2(9), (2011) 1099-1105.

2. A. Horvath, G. Weiser, G. L. Baker, S. Etemad, Influence of Disorder on the Field-modulated Spectra of Polydiacetylene films, *Phys. Rev. B* 51(5), (1995) 2751.

3. M. G. Harrison, S. Möller, G. Weiser, G. Urbasch, R. F. Mahrt, H. Bässler, U. Scherf, Electro-optical Studies of a Soluble Conjugated Polymer with Particularly Low Intrachain Disorder, *Phys. Rev. B* 60(12), (1999) 8650.

4. A. Ojala, A. Petersen, A. Fuchs, R. Lovrincic, C. Pölking, J. Trollmann, J. Hwang, C. Lennartz, H. J. Reichelt, H. W. Höffken *et al*., Merocyanine/C60 Planar Heterojunction Solar Cells: Effect of Dye Orientation on Exciton Dissociation and Solar Cell Performance, *Adv. Funct. Mat.* 22(1), (2012) 86-96.

5. D. Peckus, A. Devižis, R.Augulis, S. Graf, D. Hertel, K. Meerholz, V. Gulbinas, Charge Transfer States in Merocyanine Neat Films and Its Blends with [6, 6]-Phenyl-C61-butyric Acid Methyl Ester, *J. Phys. Chem. C* 117(12), (2013) 6039-6048.